Pharmaceutical Research, Vol. 23, No. 7, July 2006 (© 2006)
DOI: 10.1007/s11095-006-0208-7

Featured Article

Major Involvement of Low-Density Lipoprotein Receptor-Related Protein 1 in the Clearance of Plasma Free Amyloid β-Peptide by the Liver

Chihiro Tamaki,[1] Sumio Ohtsuki,[1,2,3] Takeshi Iwatsubo,[4] Tadafumi Hashimoto,[4] Kaoru Yamada,[4] Chiori Yabuki,[4] and Tetsuya Terasaki[1,2,3,5]

Received December 6, 2005; accepted February 8, 2006

Purpose. To identify the molecules responsible for amyloid β-peptide (1–40) (Aβ(1–40)) uptake by the liver, which play a major role in the systemic clearance of Aβ(1–40).
Methods. The liver uptake index method was used to examine the mechanisms of Aβ(1–40) uptake by the liver *in vivo*.
Results. [^{125}I]Aβ(1–40) uptake by the rat liver was concentration-dependent (50% saturation concentration = 302 nM). The inhibitory spectrum of Aβ fragments indicated that 17–24 in Aβ (LVFFAEDV) was the putative sequence responsible for hepatic Aβ(1–40) uptake. Receptor-associated protein (RAP) inhibited [^{125}I]Aβ(1–40) uptake by 48%. RAP-deficient mice, in which low-density lipoprotein receptor-related protein 1 (LRP-1) expression was suppressed, showed a 46% reduction in [^{125}I]Aβ(1–40) uptake by the liver. siRNA-mediated suppression of LRP-1 expression in the liver resulted in a reduction in [^{125}I]Aβ(1–40) uptake by 64%. Both the expression of LRP-1 in the liver and the hepatic Aβ(1–40) uptake were significantly reduced in 13-month-old rats compared with 7-week-old rats.
Conclusions. LRP-1 is the major receptor responsible for the saturable uptake of plasma free Aβ(1–40) by the liver. Reduction of LRP-1 expression will play a role in the age-related reduction in hepatic Aβ(1–40) clearance.

KEY WORDS: amyloid β-peptide; clearance; liver uptake index; low-density lipoprotein receptor-related protein 1; receptor-mediated endocytosis.

INTRODUCTION

Amyloid β-peptide (Aβ), a 39- to 43-amino-acid peptide derived from the proteolytic cleavage of amyloid precursor protein, is the main constituent of brain parenchymal and cerebrovascular amyloid deposits in Alzheimer's disease (AD). The 40-amino-acid form of Aβ, Aβ(1–40), is the predominant form of cerebrovascular amyloid (1), accounting for approximately 90% of soluble monomeric Aβ produced by different cell types (2) and normally present in the circulation (3).

Under physiological conditions, plasma Aβ(1–40) is mainly associated with albumin and lipoproteins (4), and is rapidly cleared from the circulation. Intravenously injected Aβ(1–40) is eliminated from the circulation in a saturable manner with a half-life of 1.2–15 min in rodents (5–8). Recent studies have revealed that this rapid clearance of plasma Aβ(1–40) is largely mediated by the liver, accounting for 40–60% of the total uptake, followed by the kidney (6,7).

Systemic clearance of Aβ(1–40) has been shown to play a role in determining the levels of plasma Aβ(1–40) available for transport into the brain (9,10). Increased levels of plasma Aβ, leading to cerebrovascular Aβ deposition, are frequently found in elderly individuals (11). In the squirrel monkey, a well-established nonhuman primate model of cerebrovascular amyloid angiopathy (CAA), systemic clearance of Aβ(1–40) decreases with age (9), indicating that attenuation of systemic Aβ(1–40) clearance may increase plasma Aβ levels and enhance the development of CAA. Thus, strategies focused on the modulation of systemic clearance of Aβ seem to be effective for the development of new therapeutic approaches for preventing cerebrovascular Aβ deposition.

[1] Department of Molecular Biopharmacy and Genetics, Graduate School of Pharmaceutical Sciences, Tohoku University, Aoba, Aramaki, Aoba-ku, Sendai 980-8579, Japan.
[2] New Industry Creation Hatchery Center, Tohoku University, Aoba, Aramaki, Aoba-ku, Sendai 980-8579, Japan.
[3] SORST of Japan Science and Technology Agency (JST), Japan.
[4] Department of Neuropathology and Neuroscience, Graduate School of Pharmaceutical Sciences, University of Tokyo, 7-3-1 Hongo, Bunkyoku, Tokyo 113-0033, Japan.
[5] To whom correspondence should be addressed. (e-mail: terasaki@mail.pharm.tohoku.ac.jp)

ABBREVIATIONS: Aβ, amyloid β-peptide; AD, Alzheimer's disease; AGEs, advanced glycation end products; apoE, apolipoprotein E; BBB, blood–brain barrier; BSA, bovine serum albumin; CAA, cerebrovascular amyloid angiopathy; FITC, fluorescein-4-isothiocyanate; LDL, low-density lipoprotein; LRP-1, LDL receptor-related protein 1; LUI, liver uptake index; RAGE, receptor for AGEs; RAP, receptor-associated protein; SDS, sodium dodecylsulfate; siRNA, short interfering RNA; SR-A, scavenger receptor type A.

Although recent advances highlight the importance of plasma Aβ(1–40) clearance, especially by the liver, the molecular mechanisms of the hepatic Aβ(1–40) uptake are still poorly understood. A previous study has reported that the hepatic uptake of Aβ(1–40) was absent in apolipoprotein E (apoE)-deficient mice (6). ApoE is a plasma lipoprotein that directly binds Aβ(1–40) (12), and is a ligand of low-density lipoprotein (LDL) receptor-related protein 1 (LRP-1) (13). Both free and apoE-associated Aβ(1–40) in the brain are transported to the circulation across the blood–brain barrier (BBB) via LRP-1-mediated endocytosis (14,15). It is possible that an LRP-1-mediated uptake process for free Aβ(1–40) and/or Aβ(1–40) associated with plasma proteins is also present in the liver, where LRP-1 is highly expressed (16).

The purpose of the present study was to identify the molecules responsible for the hepatic uptake of Aβ(1–40). The mechanisms by which plasma Aβ(1–40) is transported into the liver were investigated by using the liver uptake index (LUI) method (17), in which [^{125}I]Aβ(1–40) was rapidly injected into a portal vein. This LUI measurement mainly reflects the uptake of free Aβ(1–40) by the liver.

MATERIALS AND METHODS

Animals

Sprague-Dawley rats, C57BL/6J mice, and ICR mice were supplied by Charles River (Yokohama, Japan). Receptor-associated protein (RAP)-deficient mice (Stock #002987) were obtained from Jackson Laboratory (Bar Harbor, ME, USA). All animals were allowed *ad libitum* access to tap water and a pelleted diet (CRF-1; Charles River). The investigations described in this report conformed to the requirements of the Animal Care Committee, Graduate School of Pharmaceutical sciences, Tohoku University, Japan.

Reagents

[^{125}I]Aβ(1–40) (2,200 Ci/mmol) and [^{3}H]water (1 mCi/g) were purchased from Perkin-Elmer Life Sciences (Boston, MA, USA). Unlabeled Aβ peptides and fragments were purchased from Bachem AG (Bubendorf, Switzerland) except Aβ(1–40). Aβ(1–40) and fluorescein-4-isothiocyanate (FITC)-Aβ(1–40) were purchased from Sigma (St. Louis, MO, USA) and Anaspec (San Jose, CA, USA), respectively. Human recombinant insulin, fucoidan from *Fucus vesiculosus*, and xylazine hydrochloride were purchased from Sigma. Ketamine hydrochloride was purchased from Sankyo (Tokyo, Japan). RAP was purchased from Oxford Biomedical Research (Oxford, MI, USA). Advanced glycation end products (AGEs) were prepared by incubating bovine serum albumin (BSA) with D-ribose, as previously described (18). The same procedure, but without D-ribose, was used to prepare a control BSA. All other chemicals were commercial products of reagent grade.

Liver Uptake Index Method

The unidirectional uptake of plasma Aβ(1–40) by the liver was determined by injecting [^{125}I]Aβ(1–40) into a portal vein, as previously described (17,19). Rats were anesthetized by intramuscular injection of ketamine (125 mg/kg) and xylazine (1.25 mg/kg), and their rectal temperatures were maintained at 37°C by using a hot plate. The hepatic artery was ligated, and 200 μL Ringer's HEPES buffer (pH 7.4), which contained both 0.2 μCi [^{125}I]Aβ(1–40) and 4.0 μCi [^{3}H]water as a highly diffusible internal reference, was rapidly injected into the portal vein. Eighteen seconds after injection, the right major lobe was excised from the liver and solubilized in Solvable (Packard Instruments, Meriden, CT, USA). Levels of ^{125}I and ^{3}H in the liver and in the injection solutions were measured by using a gamma counter (ALC300; Aloca, Tokyo, Japan) and a liquid scintillation counter (TRI-CARB 2050CA; Packard Instruments), respectively. When using mice, ligation of the hepatic artery was omitted, the volume of solution injected was reduced to 100 μL and the interval after the injection was reduced to 5 s, as previously described (19).

Determination of the LUI

LUI is defined in Eq. (1), and was determined by using Eq. (2):

$$LUI = E_T/E_R \tag{1}$$

$$LUI(\%) = \left(\left[^{125}\mathrm{I}\right]/\left[^{3}\mathrm{H}\right]\right)\text{counts in the liver}/\left(\left[^{125}\mathrm{I}\right]/\left[^{3}\mathrm{H}\right]\right)\text{counts in the injection solution} \times 100 \tag{2}$$

Here, E_T and E_R are the fractions of [^{125}I]Aβ(1–40) and [^{3}H]water, respectively, extracted by the liver on a single pass. The value of E_T can be estimated when *LUI* and E_R are determined experimentally. Because the E_R value of [^{3}H]water is reported as 65 ± 4 and 50 ± 4% in rats and mice, respectively (17,19), the following equation is valid:

$$E_T = (LUI) \times (0.65 \text{ or } 0.50) \tag{3}$$

Estimation of Kinetic Parameters

The apparent fractional extractions consist of intracellular uptake, distribution to the interstitial space, and retention in the vascular space. Therefore, the extravascular extraction of [^{125}I]Aβ(1–40) (E), which is only due to the intracellular uptake, was obtained as follows:

$$E = (E_T - E_{ns})/(100 - E_{ns}) \tag{4}$$

Here, E_{ns} represents the fractional extraction for distribution in the vascular and extracellular space. In this calculation, we used the reported E_{ns} value of 13 ± 3 and 5.6 ± 1.3% for rats and mice, respectively (17,19).

The intracellular uptake rate of Aβ(1–40) [J; nmol/(min · g liver)] was determined as follows:

$$J = E \times F \times C_{in} \tag{5}$$

Here, F and C_{in} are the portal blood flow rate and the concentration in the injection solution. In this calculation, we

used the reported portal blood flow of 1.4 and 3.7 mL/(min · g liver) for rats and mice, respectively (17,19). To estimate the kinetic parameters of Aβ(1–40) uptake, the intracellular uptake rate was fitted to the following equation, consisting of both a saturable and a nonsaturable linear term, by using the nonlinear least-squares regression analysis program, MULTI (21):

$$J = J_{max} \times C'/(K_t + C') + K_d \times C' \quad (6)$$

Here, J_{max} is the maximal uptake rate [nmol/(min · g liver)], K_t is the 50% saturation concentration (μM), K_d is the nonsaturable uptake rate constant [mL/(min · g liver)], and C' is the mean capillary concentration (μM). As the capillary concentration cannot approximate the concentration of the injection solution when the extravascular extraction exceeds 35%, as in this case, C' was used for the estimation of kinetic parameters (20). C' was determined as follows:

$$C' = C_{in} \times (-E)/\ln(1 - E) \quad (7)$$

The fitted line was converted to the J/C' *vs.* J form to obtain an Eadie-Hofstee plot.

Denaturing Gel Electrophoresis and Autoradiography

The integrity of [^{125}I]Aβ(1–40) in the injection solution was determined by sodium dodecylsulfate (SDS)-polyacrylamide gel electrophoresis. The injection solution containing [^{125}I]Aβ(1–40) was electrophoresed under nonreducing conditions on 16.5% Tris/tricine SDS-polyacrylamide gel (Bio-Rad, Hercules, CA, USA). After electrophoresis, gels were dried and exposed to X-Omat films (Eastman Kodak, Rochester, NY, USA) for 2 days.

FITC-Aβ(1–40) Internalization by Primary Cultured Hepatocytes

Hepatocytes were isolated from 7-week-old male Sprague-Dawley rats by a two-step *in situ* collagenase-perfusion method (22), which routinely yielded cells with a viability greater than 95%. Cells were seeded onto chamber slides coated with rat tail collagen type I (Iwaki, Chiba, Japan) in HepatoZYME-SFM (Invitrogen, Carlsbad, CA, USA) supplemented with 2 mM L-glutamine, and were harvested in a humidified atmosphere of 5% CO_2 in air at 37°C for 48 h. Cells were washed with extracellular fluid buffer (122 mM NaCl, 25 mM $NaHCO_3$, 3 mM KCl, 1.4 mM $CaCl_2$, 1.2 mM $MgSO_4 \cdot 7H_2O$, 0.4 mM K_2HPO_4, 10 mM D-glucose, 10 mM HEPES, pH 7.4, 290 mOsm/kg) and incubated with 10 μM FITC-Aβ(1–40) or FITC (Sigma) at 37°C for the times given. Cells were washed with ice-cold extracellular fluid buffer and fixed with 4% formaldehyde in 0.1 M phosphate buffer (pH 7.4). The nuclei were stained with 1.5 μM propidium iodide (Molecular Probes, Eugene, OR, USA). Cells were analyzed by using a laser scanning confocal fluorescence microscope (TCS SP; Leica, Heidelberg, Germany).

siRNA Treatment of Mice

Eleven-week-old male ICR mice were used for short interfering RNA (siRNA) experiments to reduce the amount of reagents needed. siRNA targeted to the coding region of LRP-1 mRNA [NM_008512] (5′-AAC UCU CAG AAC AUC CUA GCU-3′) and its control scrambled sequence (5′-AAU GAC ACG CCU ACU ACU UAC-3′) were synthesized by Japan Bio Services Co. (Saitama, Japan). Double-stranded siRNA (5 nmol), which was generated according to the manufacturer's instructions, was dissolved in 2 mL phosphate-buffered saline and administered to mice by using the hydrodynamic tail vein injection method (23). Subsequent experiments were performed 48 h after injection.

Western Blot Analysis

Crude membrane proteins were prepared from the liver, as previously described (24). Proteins (5 μg/lane) were electrophoresed under nonreducing conditions on 7.5% Tris/glycine SDS-polyacrylamide gel (Bio-Rad). Separated proteins were subsequently electrotransferred to a nitrocellulose membrane (Toyo Roshi, Tokyo, Japan), and the membrane was treated with blocking solution (25 mM Tris, 125 mM NaCl, 5% skimmed milk, 0.1% Tween 20, pH 8.0) for 1 h and diluted antibody against β-chain of LRP-1 (0.1 μg/mL; American Diagnostica, Greenwich, CT, USA) or antibody against β-actin (1:2,000; Sigma) for 16 h at 4°C. The membrane was washed with 0.1% Tween 20 in phosphate-buffered saline and then incubated with horseradish peroxidase-conjugated anti-mouse IgG (1:5,000; ICN, Aurora, OH, USA) for 1 h. Immunoreactivity was visualized with an enhanced chemiluminescence kit (Supersignal west pico chemiluminescent substrate; Pierce, Rockford, IL, USA) and exposed to X-OmatAR films (Eastman Kodak). Densitometric images were analyzed with Scion Image Beta WIN 4.02 software (Scion Corporation, Frederick, MD, USA).

Statistical Analysis

Unless otherwise indicated, all data are presented as the mean ± SEM. Statistical significance of differences between the means was determined by using the unpaired two-tailed Student's t test for two groups and by one-way analysis of variance followed by the Dunnett's test for more than two groups.

RESULTS

Concentration Dependence of Aβ(1–40) Uptake in the Liver

In 7-week-old male Sprague–Dawley rats, the extravascular extraction of [^{125}I]Aβ(1–40) was 69.5 ± 3.1% (mean ± SEM, n = 6), indicating that 70% of the injected [^{125}I]Aβ(1–40) was taken up by the liver on a single pass. The extravascular extraction of [^{125}I]Aβ(1–40) was reduced by increasing the unlabeled Aβ(1–40) concentration in the injection solution (Fig. 1A). As shown in Fig. 1B, which plots the intracellular uptake rate (J) of Aβ(1–40) against the mean capillary concentration (C'), hepatic [^{125}I]Aβ(1–40) uptake was composed of a saturable and a nonsaturable process. Fitting these data to Eq. (6), the kinetic parameters for the saturable process were estimated as K_t = 0.302 ± 0.035 μM and J_{max} = 0.350 ± 0.039 nmol/(min · g liver), and that for the

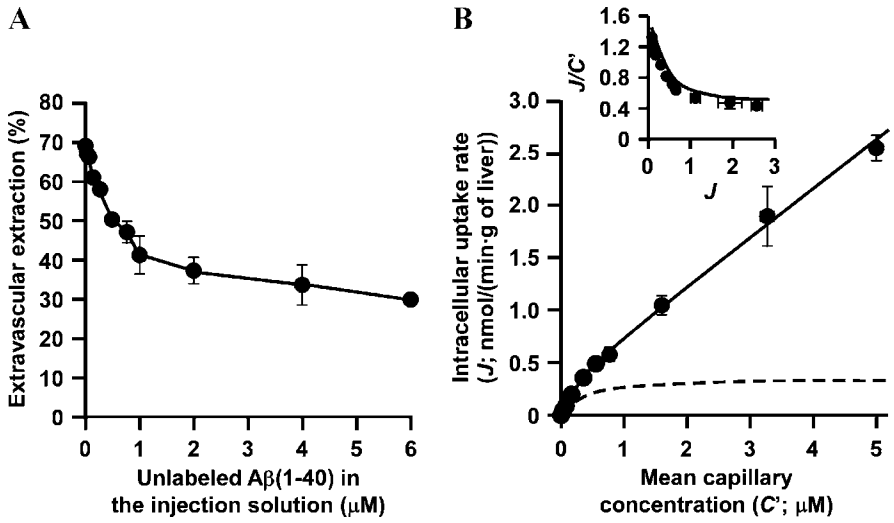

Fig. 1. Concentration-dependent uptake of Aβ(1–40) by rat liver. (A) The extravascular extraction of [^{125}I]Aβ(1–40) was plotted against the Aβ(1–40) concentration in the injection solution. (B) The intracellular uptake rate of Aβ(1–40) (J; nmol/(min · g liver)) calculated by Eq. (5) was plotted against the mean capillary concentration of Aβ(1–40) (C'; μM) calculated by Eq. (7). The solid line represents the overall uptake rate, while the dashed line represents the saturable term of the uptake in Eq. (6) and was generated from the parameters of J_{max} and K_t, which were determined by a nonlinear least-squares regression analysis of the data. Inset: Eadie-Hofstee plot of the same data. Each data point represents the mean ± SEM (n = 3–6).

nonsaturable process as K_d = 0.457 ± 0.080 mL/(min · g liver) (mean ± SD).

Time-Dependent Recovery of Aβ(1–40) Uptake in the Liver

The effect of pretreatment with unlabeled Aβ(1–40) on the hepatic uptake of [^{125}I]Aβ(1–40) was examined (Fig. 2). [^{125}I]Aβ(1–40) uptake was completely abolished by a portal injection of 10 μM unlabeled Aβ(1–40) administered 0.5 min earlier. This observation indicated the saturation of a limited number of cell-surface receptors for Aβ(1–40) in the liver. The uptake of [^{125}I]Aβ(1–40) gradually recovered as the time interval between the initial injection of the unlabeled Aβ(1–40) and the second injection of [^{125}I]Aβ(1–40) increased, with a rate constant (k) of 6.57 × 10^{-2} min^{-1} and a half-life ($t_{1/2}$) of 10.5 min. This time-dependent recovery reflected the recycling of receptors responsible for Aβ(1–40) uptake in the liver.

Internalization of FITC-Aβ(1–40) by Primary Cultured Hepatocytes

When FITC-Aβ(1–40) was incubated with primary cultured rat hepatocytes at 37°C, green fluorescence derived from FITC-Aβ(1–40) was detected in the cytoplasmic compartment of the hepatocytes (Fig. 3). Fluorescence intensity increased in a time-dependent manner, and maximal fluorescence was reached after 30–60 min of treatment. No significant fluorescence was observed in hepatocytes over the same period when FITC was used as a negative control.

Sequence Selectivity of Aβ(1–40) Uptake in the Liver

The hepatic uptake of [^{125}I]Aβ(1–40) was significantly inhibited not only in the presence of unlabeled Aβ(1–40) but also in the presence of Aβ(1–42), a peptide that is two amino acids longer, by 64 and 24%, respectively (Fig. 4A). However, a peptide that was three amino acids longer, Aβ(1–43), and the reverse sequences, Aβ(40–1) and Aβ(42–1), had no significant effect on [^{125}I]Aβ(1–40) uptake. To identify the putative sequence responsible for Aβ(1–40) uptake by the liver, the inhibitory effect of various Aβ fragments

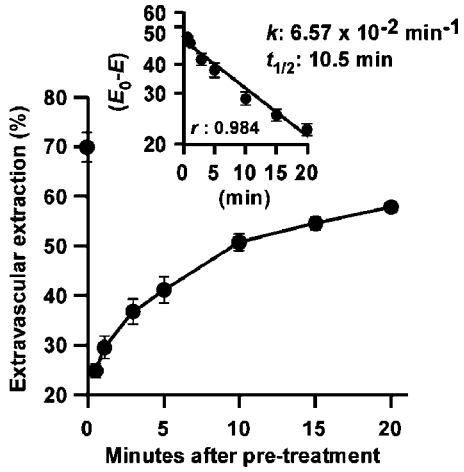

Fig. 2. Time-dependent recovery of Aβ(1–40) uptake in rat liver. The extravascular extraction of [^{125}I]Aβ(1–40) was determined after pretreatment with 10 μM unlabeled Aβ(1–40), and the time between the first (unlabeled Aβ(1–40)) and second injections ([^{125}I]Aβ(1–40)) varied from 0.5 to 20 min. Inset: log(E_0 − E), where E_0 and E represent the extravascular extraction of [^{125}I]Aβ(1–40) after injecting 0 or 10 μM unlabeled Aβ(1–40), respectively, plotted against the time between the two injections. Each data point represents the mean ± SEM (n = 3–6). k is the rate constant and $t_{1/2}$ is the half-life for the recovery of [^{125}I]Aβ(1–40) uptake.

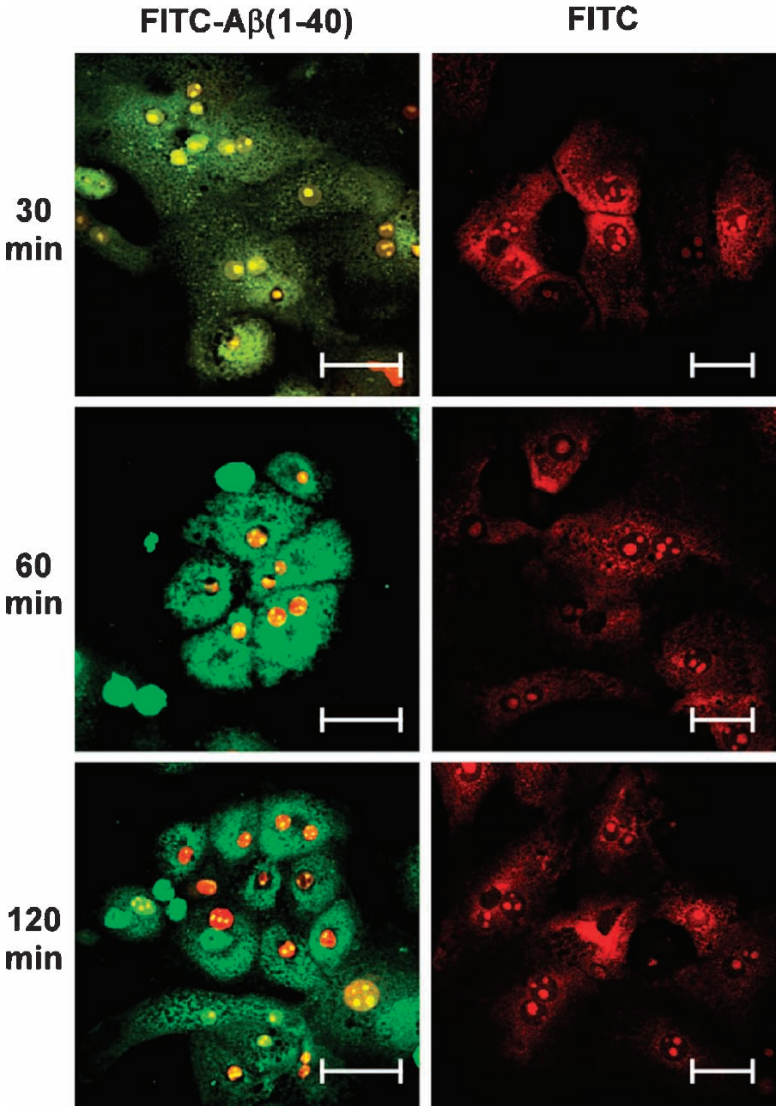

Fig. 3. Internalization of FITC-Aβ(1–40) by primary cultured rat hepatocytes. A 10-μM dose of FITC-Aβ(1–40) or FITC was incubated with hepatocytes for the indicated times at 37°C. FITC labeling is green and propidium iodide labeling of the nuclei is red. Scale bar = 50 μm.

on [^{125}I]Aβ(1–40) uptake was determined (Fig. 4B). [^{125}I]Aβ(1–40) uptake was significantly inhibited in the presence of Aβ(1–28), Aβ(12–28), and Aβ(17–40) by 42, 37, and 15%, respectively, whereas Aβ(1–11), Aβ(1–16), and Aβ(25–35) had no significant effect on the uptake. The pattern of inhibition observed with different Aβ fragments indicated that amino acids 17–24 (LVFFAEDV) in Aβ were responsible for its recognition by the receptor in the liver (Fig. 4E).

Because synthetic Aβ is highly amyloidogenic under physiological conditions, the integrity of [^{125}I]Aβ(1–40) in the injection solution was determined by autoradiography. Under the experimental conditions used, [^{125}I]Aβ(1–40) was exclusively monomeric, appearing as a major band of 4 kDa (Fig. 4C; control). Little or no aggregation of [^{125}I]Aβ(1–40) was observed by adding excess of unlabeled Aβ peptides or fragments to the injection solution (Fig. 4C, D).

Effect of Insulin, Fucoidan, AGEs, and RAP on the Hepatic Uptake of Aβ(1–40)

The hepatic uptake of [^{125}I]Aβ(1–40) was not affected by insulin or fucoidan, which is a scavenger receptor type A (SR-A) ligand (Table I). AGEs, model ligands for receptor for AGEs (RAGE), inhibited [^{125}I]Aβ(1–40) uptake by 15%, whereas control BSA had no significant effect. RAP, which inhibits ligand binding to the LDL receptor gene family, significantly inhibited [^{125}I]Aβ(1–40) uptake by 48%.

Involvement of LRP-1 in the Uptake of Aβ(1–40) in the Liver

To clarify the involvement of LRP-1, the hepatic uptake of Aβ(1–40) was examined under conditions of LRP-1 suppression: RAP-deficient mice and LRP-1 siRNA treat-

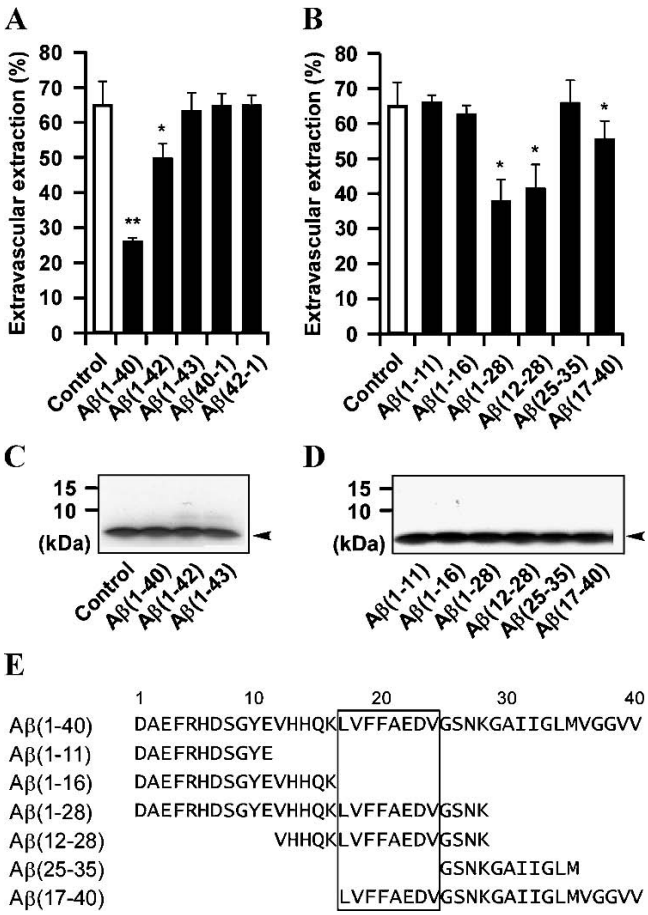

Fig. 4. Sequence-selective uptake of Aβ(1–40) by rat liver. (A, B) The extravascular extraction of [^{125}I]Aβ(1–40) was determined in the presence of 20 μM Aβ peptides (A) or fragments (B). Each column represents the mean ± SEM (n = 4–6). Significant differences from controls are indicated by asterisks: *$p < 0.05$, **$p < 0.01$. (C, D) SDS-polyacrylamide gel electrophoresis showing [^{125}I]Aβ(1–40) in the presence of Aβ peptides (C) or fragments (D). The sizes of the monomeric [^{125}I]Aβ(1–40) are indicated by arrowheads. (E) The sequences of different Aβ fragments were compared and the putative sequence responsible for Aβ(1–40) recognition is shown by a box.

ment. LRP-1 expression in 8-week-old RAP-deficient mice was significantly lower, compared with age-matched C57BL/6J control mice (Fig. 5A). The extravascular extraction of [^{125}I]Aβ(1–40) in control mice was 29.4 ± 4.6% (Fig. 5B). In RAP-deficient mice, the extravascular extraction of [^{125}I]Aβ(1–40) was 46% lower than in control mice. The intracellular uptake rate (J) of [^{125}I]Aβ(1–40) in control mice calculated from Eq. (5) was 0.467 ± 0.089 pmol/(min · g liver), which is close to that in 7-week-old male rats [0.483 ± 0.022 pmol/(min · g liver)].

In 11-week-old male ICR mouse liver, LRP-1 and β-actin protein was detected at 85 and 42 kDa, respectively, by Western blot analysis (Fig. 5C). By treating mice with LRP-1 siRNA, the expression of this protein in the liver fell by 77%, compared with saline-injected mice, whereas scrambled siRNA had no significant effect on LRP-1 expression. The level of β-actin protein was not affected by treatment with either siRNA. LRP-1 siRNA significantly reduced [^{125}I]Aβ(1–40) uptake by 64%, compared with saline-injected mice, whereas scrambled siRNA had no significant effect on the uptake (Fig. 5D).

Effect of Age on LRP-1 Expression in the Liver and the Hepatic Uptake of Aβ(1–40)

Levels of LRP-1 protein expression in the liver of 7-week-old and 13-month-old rats were determined by Western blot analysis. LRP-1 and β-actin protein were detected at 85 and 42 kDa, respectively, in rat liver, which agrees with the mouse results. LRP-1 expression in the liver of 13-month-old rats was 39% lower in males and 26% lower in females, compared with 7-week-old rats (Fig. 6A). The level of β-actin protein was not changed in either 7-week-old or 13-month-old rats. The extravascular extraction of [^{125}I]Aβ(1–40) in 13-month-old rats was 24% lower in males and 26% lower in females, compared with 7-week-old rats (Fig. 6B). At both 7 weeks and 13 months of age, there were no significant gender differences in either LRP-1 expression or [^{125}I]Aβ(1–40) uptake.

DISCUSSION

The liver is the major organ responsible for the clearance of Aβ(1–40) from the circulation. Using the LUI method, we demonstrated that LRP-1-mediated endocytosis is the major pathway for the uptake of plasma free Aβ(1–40) by the liver. The hepatic uptake of Aβ(1–40) was concentration-dependent and composed of a saturable and a non-saturable process (Fig. 1). K_t for the saturable process of Aβ(1–40) uptake was 0.302 μM, which is more than 1,500-fold greater than the physiological Aβ(1–40) levels in plasma, reported previously, i.e., 30–200 pM (25). Employing these values and Eq. (6), it seems that the saturable process of Aβ(1–40) uptake is unlikely to reach saturation, and the contribution of the saturable process to the total uptake is estimated to be a constant value, approximately 72%, over the physiological range of plasma Aβ(1–40) levels.

The effect of pretreatment with unlabeled Aβ(1–40) on uptake by the liver revealed the involvement of receptor-mediated endocytosis (Fig. 2). The recovery rate of labeled Aβ(1–40) uptake, representing the *in vivo* recycling rate of the receptors, had a recycling half-life of 10.5 min. This figure

Table I. Effect of Various Substrates on Aβ(1–40) Uptake by Rat Liver

Substrates	Extravascular extraction (%)	Percentage of control (%)
Control	69.5 ± 2.3	100 ± 3
100 μg/mL insulin	66.5 ± 3.4	96 ± 5
100 μg/mL fucoidan	66.8 ± 2.3	96 ± 4
1 mg/mL AGEs	59.2 ± 1.4*	85 ± 2
1 mg/mL control BSA	69.0 ± 2.7	99 ± 4
2 μM RAP	36.3 ± 3.1**	52 ± 4

AGEs, advanced glycation end products; BSA, bovine serum albumin; RAP, receptor-associated protein.
Substrates dissolved in 200 μL Ringer's HEPES buffer (pH 7.4) at the indicated concentrations were injected 0.5 min prior to [^{125}I]Aβ(1–40). Each value represents the mean ± SEM (n = 4–6). *$p < 0.05$, **$p < 0.01$, significantly different compared with controls.

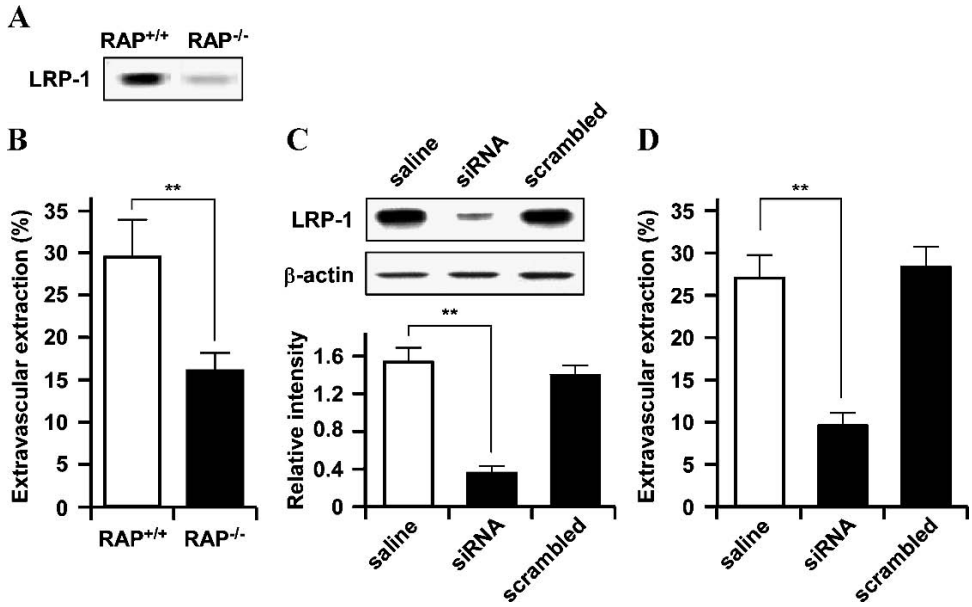

Fig. 5. Involvement of LRP-1 in the uptake of Aβ(1–40) in mouse liver. (A) The expression of LRP-1 in livers from 8-week-old C57BL/6J mice ($RAP^{+/+}$) and age-matched RAP-deficient mice ($RAP^{-/-}$) was determined by Western blot analysis. (B) The extravascular extraction of [^{125}I]Aβ(1–40) in $RAP^{+/+}$ and $RAP^{-/-}$ mice was determined. Each column represents the mean ± SEM (n = 4–5). (C) siRNA targeted to mouse LRP-1 (siRNA) or the control scrambled sequence (scrambled) was administered to 11-week-old male ICR mice using the hydrodynamic tail vein injection method. After 48 h, the expression of LRP-1 and β-actin protein in the liver was determined by Western blot analysis and the relative band intensities (LRP-1/β-actin) were determined by densitometry. Each column represents the mean ± SEM (n = 3). (D) The extravascular extraction of [^{125}I]Aβ(1–40) in siRNA-treated mice was determined. Each column represents the mean ± SEM (n = 4–6). **Significant differences compared with relevant controls, $p < 0.01$.

is similar to the reported half-life values for the internalization and externalization of another LRP-1 ligand, α-macroglobulin–trypsin complex, in rabbit alveolar macrophages, which were 3 min (26) and 2 (27) min, respectively.

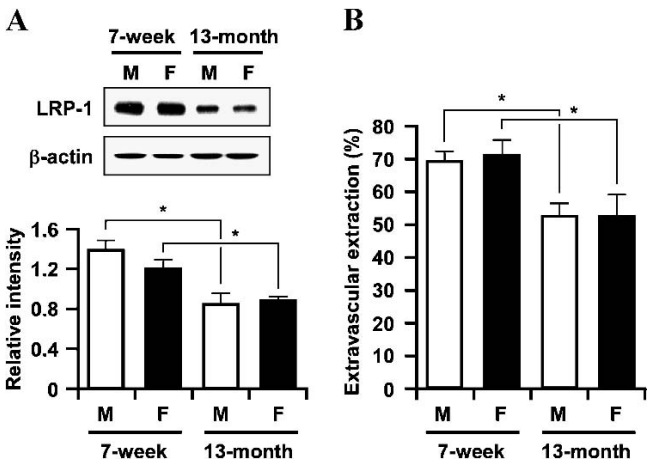

Fig. 6. Effect of age on LRP-1 expression in rat liver and the hepatic uptake of Aβ(1–40). (A) The expression of LRP-1 and β-actin proteins in livers from 7-week- and 13-month-old male (M) and female (F) rats was determined by Western blot analysis, and the relative band intensities (LRP-1/β-actin) were determined. Each column represents the mean ± SEM (n = 3). (B) The extravascular extraction of [^{125}I]Aβ(1–40) in 7-week- and 13-month-old rats was determined. Each column represents the mean ± SEM (n = 4–6). *Significant differences compared with relevant controls, $p < 0.05$.

By incubating 10 μM FITC-Aβ(1–40) with primary cultured hepatocytes, FITC-Aβ(1–40) was internalized in a time-dependent manner (Fig. 3). Because of the detection limit of FITC fluorescence, this experiment was performed under conditions in which most of the Aβ(1–40) uptake would be saturated. Although the contribution of the saturable process to the total uptake of FITC-Aβ(1–40) could be estimated via Eq. (6) as approximately 7%, particles of the intense green fluorescence in Fig. 3 shows the internalization of FITC-Aβ(1–40) by hepatocytes. No significant fluorescence was observed by incubating FITC, which excludes the possibility that a time-dependent increase in fluorescence reflects the internalization of FITC degraded from intact FITC-Aβ(1–40). This *in vitro* result indicates that *in vivo* LUI measurements reflected not only the binding of Aβ(1–40) to the cell surfaces but also its intracellular uptake. Degradation has been reported to be the major mechanism for the uptake of Aβ(1–40) in the liver (7). Therefore, the diffused fluorescence seen in the cytoplasmic compartment of hepatocytes would be due to degradation and/or release of FITC-Aβ(1–40) into the cytosol after internalization.

The hepatic uptake of Aβ(1–40) was sequence-dependent, and sensitive to Aβ(1–42) but not to Aβ(1–43) (Fig. 4A). The pattern of inhibition shown by different Aβ fragments (Fig. 4B) indicated that the relatively hydrophobic sequence, 17–24 in Aβ (LVFFAEDV), was the putative sequence responsible for receptor recognition (Fig. 4E). Although Aβ(1–40), Aβ(1–42), and Aβ(1–43) share the amino acid sequence of 17–24 in Aβ, inhibitory effects on the uptake were

different among these three peptides (Fig. 4A). It is conceivable that the change in the secondary structure due to the length of the carboxyl terminus affects the interaction between receptor(s) and the recognition sequence in Aβ, because the carboxyl terminus of Aβ has been reported to influence its secondary structure (28) and the rate of amyloid formation (29). It was also possible that the inhibitory effects shown in Fig. 4A and B resulted from the enhancement of insoluble oligomer formation. However, as shown in Fig. 4C and D, [^{125}I]Aβ(1–40) was exclusively monomeric under the experimental conditions used, indicating that the inhibitory effect of unlabeled Aβ on the uptake shown in Fig. 4A and B is a result of competitive inhibition on Aβ receptors, and not of oligomer formation.

The putative sequence responsible for receptor recognition in the liver is different from those previously identified for Aβ receptors, including α5β1 integrin and serine proteinase inhibitor–enzyme complex receptor, which recognize amino acids 5–8 and 31–35 in Aβ, respectively (30,31). The insulin receptor has been reported to bind Aβ(1–40) at amino acids 16–25, which is similar to the sequence responsible for Aβ(1–40) recognition in the liver (32). However, insulin did not inhibit Aβ(1–40) uptake by the liver (Table I). Considering all these findings, α5β1 integrin, serine proteinase inhibitor–enzyme complex receptors, and insulin receptors are not responsible for the hepatic uptake of Aβ(1–40). Amino acids 17–24 in Aβ could be a novel sequence involved in the receptor recognition in the liver.

To better understand the receptors responsible for Aβ(1–40) uptake in the liver, the receptors implicated in Aβ binding and transport at the BBB were examined (Table I). At the luminal side of the BBB, SR-A and RAGE mediate the binding of Aβ(1–40), and RAGE is also involved in the uptake of plasma Aβ(1–40) (33,34). Although SR-A and RAGE are expressed in the liver, the lack of inhibition by fucoidan and the moderate inhibition by AGEs indicated no role for SR-A and only a minor involvement of RAGE in Aβ(1–40) uptake by the liver.

LRP-1, a member of the LDL receptor gene family, is expressed in a variety of tissues including the liver and the brain (16), and mediates the internalization and degradation of ligands (13). Recent studies suggest that LRP-1 is involved in the brain-to-blood clearance of Aβ(1–40) associated with LRP-1 ligands, such as apoE and α2-macroglobulin (14,35), and also in the clearance of free Aβ(1–40) (15). RAP is a chaperone molecule that facilitates the trafficking of the LDL receptor gene family to the membrane and also inhibits ligand binding to the receptors (36). The inhibition of Aβ(1–40) uptake by RAP (48%; Table I) suggests major involvement of the LDL receptor gene family in the hepatic uptake of Aβ(1–40).

RAP-deficient mice have been used for characterizing LRP-1 function *in vivo*, as germline disruption of the LRP-1 gene exhibited early embryonic lethality (37) and deletion of the RAP gene results in reduced expression of the LDL receptor gene family, relatively specific to LRP-1 (38,39). As shown in Fig. 5A and B, the hepatic uptake of Aβ(1–40) was reduced in RAP-deficient mice accompanied by a reduction in LRP-1 expression in the liver. This result suggests the involvement of LRP-1 in the hepatic uptake of Aβ(1–40), whereas suppression effects of the RAP gene deficient on other LDL receptor gene families could not be ruled out. Therefore, siRNA targeted to the LRP-1-specific sequences, which does not have homologies with other LDL receptor gene families including LDL receptors, LRP-2/gp330/megalin, and very low-density lipoprotein receptors, was designed for specific suppression of LRP-1. LRP-1 expression in the liver was significantly suppressed by siRNA treatment and was correlated with a reduction in Aβ(1–40) uptake by at least 64% (Fig. 5C, D), indicating a significant involvement of LRP-1 in the Aβ(1–40) uptake by the liver. In this study, no obvious morphological changes were observed in the liver following siRNA treatment. A previous study reported that liver-specific conditional knockdown of LRP-1 using a Cre/loxP recombination system had no obvious negative effects on the apparent general health of animals, and also did not alter the plasma lipoprotein composition (40). Thus, a reduction in hepatic Aβ(1–40) uptake by siRNA treatment could be a direct result of suppressing LRP-1 expression. It is conceivable that a reduction in LRP-1 expression causes the increased plasma levels of endogenous mouse/rat Aβ(1–40), which differs from the human sequence by three amino acids (R5G, Y10F, and H13R). Mouse/rat Aβ(1–40) shares the putative sequence responsible for receptor recognition (amino acids 17–24 in Aβ) and could inhibit LRP-1-mediated Aβ(1–40) uptake by the liver. If the endogenous plasma Aβ(1–40) levels under conditions of LRP-1 suppression increased to 0.03 μM, i.e., one tenth of the K_t for the saturable uptake process, the increased endogenous Aβ(1–40) in plasma, which is 150-fold greater than that under physiological conditions, would reduce the hepatic uptake of [^{125}I]Aβ(1–40), resulting in an overestimation of the LRP-1 suppression effect.

Increased levels of plasma Aβ(1–40) are frequently found in elderly individuals (11), and systemic clearance of Aβ(1–40) decreases with age in the squirrel monkey (9). The present study demonstrated that the hepatic uptake of Aβ(1–40) was attenuated in aged rats (Fig. 6). This result suggests that age-dependent attenuation of hepatic Aβ(1–40) uptake plays a role in increasing plasma Aβ levels in elderly individuals due to insufficient systemic clearance. Reduction of LRP-1 expression in aged rat liver shown in Fig. 6 would be involved in the reduced hepatic Aβ(1–40) uptake at least in part, whereas hepatic aging including decreased tissue mass, lean mass, or lysosomal activities may also have an effect on the hepatic uptake of Aβ(1–40).

The present study has demonstrated the rapid uptake of plasma free Aβ(1–40) via LRP-1-mediated endocytosis by the liver, whereas plasma Aβ(1–40) is mainly associated with albumin and lipoproteins (4). In the LUI method, there would be a mixing of circulating plasma with injected Aβ(1–40), at least in part, after the rapid portal vein injection. The degree of blood mixing with the injection solution after the rapid portal vein injection has not been reported, although we may consider 5% as the mixing reported for the brain uptake index method (41). Thus, the LUI measurements reflect mainly the uptake of free Aβ(1–40) by the liver, although we cannot exclude the possibility that Aβ(1–40), in part associated with plasma proteins such as lipoproteins, is taken up into the liver. It is possible that lipoprotein-associated plasma Aβ(1–40) is also taken up into the liver by LRP-1-mediated endocytosis as

well as free Aβ(1–40), because LRP-1 interacts with Aβ(1–40) both directly and via LRP-1 ligands (14,15,35). The reduction in hepatic Aβ(1–40) uptake in apoE-deficient mice (6) could be explained by the hypothesis that, in the absence of apoE, Aβ(1–40) binds to other plasma proteins, and not LRP-1 ligands such as albumin, leading to a reduction in LRP-1-mediated Aβ(1–40) uptake. Systemic administration of antibodies against Aβ has been reported to reduce Aβ deposition in the brain of AD model mice, and this could be a potential vaccine therapy for AD (42). After administration of the antibodies, a rapid increase in the plasma Aβ levels occurs (43), and this leads to an increase in cerebrovascular amyloid (44). This increase also seems to be partly the result of a reduction in hepatic Aβ(1–40) uptake due to antibodies capturing Aβ in the circulation.

In conclusion, the present study demonstrates that LRP-1 is the major receptor involved in the clearance of plasma free Aβ(1–40) by the liver, and the age-dependent attenuation of hepatic Aβ(1–40) clearance is attributable to, at least in part, reduced hepatic LRP-1 expression. The present findings will be important to further increase our understanding of the role of hepatic clearance in the modulation of plasma Aβ(1–40) levels.

ACKNOWLEDGMENTS

We would like to thank Dr. T. Yokota for valuable discussions, and Ms. N. Funayama for secretarial assistance. This study was supported in part by a Grant-in-Aid for Scientific Research on Priority Areas 17025005 from The Ministry of Education, Culture, Sports, Science and Technology (MEXT), Japan, and a 21st Century Center of Excellence (COE) Program grant from the Japan Society for the Promotion of Science.

REFERENCES

1. E. M. Castano, F. Prelli, C. Soto, R. Beavis, E. Matsubara, M. Shoji, and B. Frangione. The length of amyloid-beta in hereditary cerebral hemorrhage with amyloidosis, Dutch type. Implications for the role of amyloid-beta 1–42 in Alzheimer's disease. *J. Biol. Chem.* **271**:32185–32191 (1996).
2. M. Citron, T. S. Diehl, G. Gordon, A. L. Biere, P. Seubert, and D. J. Selkoe. Evidence that the 42- and 40-amino acid forms of amyloid beta protein are generated from the beta-amyloid precursor protein by different protease activities. *Proc. Natl. Acad. Sci. USA* **93**:13170–13175 (1996).
3. P. Seubert, C. Vigo-Pelfrey, F. Esch, M. Lee, H. Dovey, D. Davis, S. Sinha, M. Schlossmacher, J. Whaley, C. Swindlehurst, R. Mccormack, R. Wolfert, D. J. Selkou, I. Lieberburg, and D. Schenk. Isolation and quantification of soluble Alzheimer's beta-peptide from biological fluids. *Nature* **359**:325–327 (1992).
4. A. L. Biere, B. Ostaszewski, E. R. Stimson, B. T. Hyman, J. E. Maggio, and D. J. Selkoe. Amyloid beta-peptide is transported on lipoproteins and albumin in human plasma. *J. Biol. Chem.* **271**:32916–32922 (1996).
5. J. F. Poduslo, G. L. Curran, J. J. Haggard, A. L. Biere, and D. J. Selkoe. Permeability and residual plasma volume of human, Dutch variant, and rat amyloid beta-protein 1-40 at the blood–brain barrier. *Neurobiol. Dis.* **4**:27–34 (1997).
6. E. Hone, I. J. Martins, J. Fonte, and R. N. Martins. Apolipoprotein E influences amyloid-beta clearance from the murine periphery. *J. Alzheimer's Dis.* **5**:1–8 (2003).
7. J. Ghiso, M. Shayo, M. Calero, D. Ng, Y. Tomidokoro, S. Gandy, A. Rostagno, and B. Frangione. Systemic catabolism of Alzheimer's Abeta 40 and Abeta 42. *J. Biol. Chem.* **279**: 45897–45908 (2004).
8. K. K. Kandimalla, G. L. Curran, S. S. Holasek, E. J. Gilles, T. M. Wengenack, and J. F. Poduslo. Pharmacokinetic analysis of the blood–brain barrier transport of ^{125}I-amyloid beta protein 40 in wild-type and Alzheimer's disease transgenic mice (APP, PS1) and its implications for amyloid plaque formation. *J. Pharmacol. Exp. Ther.* **313**:1370–1378 (2005).
9. J. B. Mackic, M. H. Weiss, W. Miao, E. Kirkman, J. Ghiso, M. Calero, J. Bading, B. Frangione, and B. V. Zlokovic. Cerebrovascular accumulation and increased blood–brain barrier permeability to circulating Alzheimer's amyloid beta peptide in aged squirrel monkey with cerebral amyloid angiopathy. *J. Neurochem.* **70**:210–215 (1998).
10. J. B. Mackic, J. Bading, J. Ghiso, L. Walker, T. Wisniewski, B. Frangione, and B. V. Zlokovic. Circulating amyloid-beta peptide crosses the blood–brain barrier in aged monkeys and contributes to Alzheimer's disease lesions. *Vascul. Pharmacol.* **38**:303–313 (2002).
11. C. C. Smith and D. J. Betteridge. Plasma beta-amyloid (A beta) 40 concentration, lipid status and age in humans. *Neurosci. Lett.* **367**:48–50 (2004).
12. W. J. Strittmatter, K. H. Weisgraber, D. Y. Huang, L. M. Dong, G. S. Salvesen, M. Pericak-Vance, D. Schmechel, A. M. Saunders, D. Goldgaber, and A. D. Roses. Binding of human apolipoprotein E to synthetic amyloid beta peptide: isoform-specific effects and implications for late-onset Alzheimer disease. *Proc. Natl. Acad. Sci. USA* **90**:8098–8102 (1993).
13. J. Herz and D. K. Strickland. LRP: a multifunctional scavenger and signaling receptor. *J. Clin. Invest.* **108**:779–784 (2001).
14. M. Shibata, S. Yamada, S. R. Kumar, M. Calero, J. Bading, B. Frangione, D. M. Holtzman, C. A. Miller, D. K. Strickland, J. Ghiso, and B. V. Zlokovic. Clearance of Alzheimer's amyloid-beta(1–40) peptide from brain by LDL receptor-related protein-1 at the blood–brain barrier. *J. Clin. Invest.* **106**:1489–1499 (2000).
15. R. Deane, Z. Wu, A. Sagare, J. Davis, S. Du Yan, K. Hamm, F. Xu, M. Parisi, B. LaRue, H. W. Hu, P. Spijkers, H. Guo, X. Song, P. J. Lenting, W. E. Van Nostrand, and B. V. Zlokovic. LRP/amyloid beta-peptide interaction mediates differential brain efflux of Abeta isoforms. *Neuron* **43**:333–344 (2004).
16. S. K. Moestrup, J. Gliemann, and G. Pallesen. Distribution of the alpha 2-macroglobulin receptor/low density lipoprotein receptor-related protein in human tissues. *Cell Tissue Res.* **269**: 375–382 (1992).
17. W. M. Pardridge and L. J. Mietus. Transport of protein-bound steroid hormones into liver *in vivo*. *Am. J. Physiol.* **237**: E367–E372 (1979).
18. J. V. Valencia, S. C. Weldon, D. Quinn, G. H. Kiers, J. DeGroot, J. M. TeKoppele, and T. E. Hughes. Advanced glycation end product ligands for the receptor for advanced glycation end products: biochemical characterization and formation kinetics. *Anal. Biochem.* **324**:68–78 (2004).
19. E. M. Cornford, L. D. Braun, W. M. Pardridge, and W. H. Oldendorf. Blood flow rate and cellular influx of glucose and arginine in mouse liver *in vivo*. *Am. J. Physiol.* **238**:H553–H560 (1980).
20. W. M. Pardridge and L. J. Mietus. Kinetics of neutral amino acid transport through the blood–brain barrier of the newborn rabbit. *J. Neurochem.* **38**:955–962 (1982).
21. K. Yamaoka, Y. Tanigawara, T. Nakagawa, and T. Uno. A pharmacokinetic analysis program (multi) for microcomputer. *J. Pharmacobio-dyn.* **4**:879–885 (1981).
22. P. O. Seglen. Preparation of isolated rat liver cells. *Methods Cell Biol.* **13**:29–83 (1976).
23. F. Liu, Y. Song, and D. Liu. Hydrodynamics-based transfection in animals by systemic administration of plasmid DNA. *Gene Ther.* **6**:1258–1266 (1999).
24. K. Wakayama, S. Ohtsuki, H. Takanaga, K. Hosoya, and T. Terasaki. Localization of norepinephrine and serotonin transporter in mouse brain capillary endothelial cells. *Neurosci. Res.* **44**:173–180 (2002).
25. M. C. Irizarry. Biomarkers of Alzheimer disease in plasma. *NeuroRx* **1**:226–234 (2004).
26. D. M. Ward and J. Kaplan. The rate of internalization of

different receptor–ligand complexes in alveolar macrophages is receptor-specific. *Biochem. J.* **270**:369–374 (1990).
27. D. M. Ward, R. Ajioka, and J. Kaplan. Cohort movement of different ligands and receptors in the intracellular endocytic pathway of alveolar macrophages. *J. Biol. Chem.* **264**:8164–8170 (1989).
28. T. Pillot, M. Goethals, B. Vanloo, C. Talussot, R. Brasseur, J. Vandekerckhove, M. Rosseneu, and L. Lins. Fusogenic properties of the C-terminal domain of the Alzheimer beta-amyloid peptide. *J. Biol. Chem.* **271**:28757–28765 (1996).
29. J. T. Jarrett, E. P. Berger, and P. T. Lansbury Jr.. The carboxy terminus of the beta amyloid protein is critical for the seeding of amyloid formation: implications for the pathogenesis of Alzheimer's disease. *Biochemistry* **32**:4693–4697 (1993).
30. G. Joslin, J. E. Krause, A. D. Hershey, S. P. Adams, R. J. Fallon, and D. H. Perlmutter. Amyloid-beta peptide, substance P, and bombesin bind to the serpin–enzyme complex receptor. *J. Biol. Chem.* **266**:21897–21902 (1991).
31. M. L. Matter, Z. Zhang, C. Nordstedt, and E. Ruoslahti. The alpha5beta1 integrin mediates elimination of amyloid-beta peptide and protects against apoptosis. *J. Cell Biol.* **141**: 1019–1030 (1998).
32. L. Xie, E. Helmerhorst, K. Taddei, B. Plewright, W. Van Bronswijk, and R. Martins. Alzheimer's beta-amyloid peptides compete for insulin binding to the insulin receptor. *J. Neurosci.* **22**:RC221 (2002).
33. J. B. Mackic, M. Stins, J. G. McComb, M. Calero, J. Ghiso, K. S. Kim, S. D. Yan, D. Stern, A. M. Schmidt, B. Frangione, and B. V. Zlokovic. Human blood–brain barrier receptors for Alzheimer's amyloid-beta 1–40. Asymmetrical binding, endocytosis, and transcytosis at the apical side of brain microvascular endothelial cell monolayer. *J. Clin. Invest.* **102**:734–743 (1998).
34. R. Deane, S. Du Yan, R. K. Submamaryan, B. LaRue, S. Jovanovic, E. Hogg, D. Welch, L. Manness, C. Lin, J. Yu, H. Zhu, J. Ghiso, B. Frangione, A. Stern, A. M. Schmidt, D. L. Armstrong, B. Arnold, B. Liliensiek, P. Nawroth, F. Hofman, M. Kindy, D. Stern, and B. Zlokovic. RAGE mediates amyloid-beta peptide transport across the blood–brain barrier and accumulation in brain. *Nat. Med.* **9**:907–913 (2003).
35. D. E. Kang, C. U. Pietrzik, L. Baum, N. Chevallier, D. E. Merriam, M. Z. Kounnas, S. L. Wagner, J. C. Troncoso, C. H. Kawas, R. Katzman, and E. H. Koo. Modulation of amyloid beta-protein clearance and Alzheimer's disease susceptibility by the LDL receptor-related protein pathway. *J. Clin. Invest.* **106**:1159–1166 (2000).
36. G. Bu. The roles of receptor-associated protein (RAP) as a molecular chaperone for members of the LDL receptor family. *Int. Rev. Cytol.* **209**:79–116 (2001).
37. J. Herz, D. E. Clouthier, and R. E. Hammer. LDL receptor-related protein internalizes and degrades uPA–PAI-1 complexes and is essential for embryo implantation. *Cell* **71**:411–421 (1992).
38. T. E. Willnow, S. A. Armstrong, R. E. Hammer, and J. Herz. Functional expression of low density lipoprotein receptor-related protein is controlled by receptor-associated protein *in vivo*. *Proc. Natl. Acad. Sci. USA* **92**:4537–4541 (1995).
39. T. E. Willnow, A. Rohlmann, J. Horton, H. Otani, J. R. Braun, R. E. Hammer, and J. Herz. RAP, a specialized chaperone, prevents ligand-induced ER retention and degradation of LDL receptor-related endocytic receptors. *EMBO J.* **15**:2632–2639 (1996).
40. A. Rohlmann, M. Gotthardt, R. E. Hammer, and J. Herz. Inducible inactivation of hepatic LRP gene by Cre-mediated recombination confirms role of LRP in clearance of chylomicron remnants. *J. Clin. Invest.* **101**:689–695 (1998).
41. W. M. Pardridge, E. M. Landaw, L. P. Miller, L. D. Braun, and W. H. Oldendorf. Carotid artery injection technique: bounds for bolus mixing by plasma and by brain. *J. Cereb. Blood Flow Metab.* **5**:576–583 (1985).
42. D. Schenk. Amyloid-beta immunotherapy for Alzheimer's disease: the end of the beginning. *Nat. Rev. Neurosci.* **3**:824–828 (2002).
43. R. B. DeMattos, K. R. Bales, D. J. Cummins, J. C. Dodart, S. M. Paul, and D. M. Holtzman. Peripheral anti-A beta antibody alters CNS and plasma A beta clearance and decreases brain A beta burden in a mouse model of Alzheimer's disease. *Proc. Natl. Acad. Sci. USA* **98**:8850–8885 (2001).
44. D. M. Wilcock, A. Rojiani, A. Rosenthal, S. Subbarao, M. J. Freeman, M. N. Gordon, and D. Morgan. Passive immunotherapy against Abeta in aged APP-transgenic mice reverses cognitive deficits and depletes parenchymal amyloid deposits in spite of increased vascular amyloid and microhemorrhage. *J. Neuroinflammation* **1**:24 (2004).